



## First-principles density functional theory study of strained wurtzite InP and InAs

Chahira Hajlaoui, Laurent Pedesseau, Faical Raouafi, F. Ben Cheikhlarbi, Jacky Even, Jean-Marc Jancu

### ► To cite this version:

Chahira Hajlaoui, Laurent Pedesseau, Faical Raouafi, F. Ben Cheikhlarbi, Jacky Even, et al.. First-principles density functional theory study of strained wurtzite InP and InAs. *Journal of Physics D: Applied Physics*, 2013, 46 (50), pp.505106. 10.1088/0022-3727/46/50/505106 . hal-00920126

**HAL Id: hal-00920126**

**<https://hal.science/hal-00920126>**

Submitted on 10 Mar 2014

**HAL** is a multi-disciplinary open access archive for the deposit and dissemination of scientific research documents, whether they are published or not. The documents may come from teaching and research institutions in France or abroad, or from public or private research centers.

L'archive ouverte pluridisciplinaire **HAL**, est destinée au dépôt et à la diffusion de documents scientifiques de niveau recherche, publiés ou non, émanant des établissements d'enseignement et de recherche français ou étrangers, des laboratoires publics ou privés.

# First-principles density functional theory study of strained wurtzite InP and InAs

C. Hajlaoui<sup>1,2</sup>, L. Pedesseau<sup>1</sup>, F. Raouafi<sup>2</sup>, F. Ben Cheikh Larbi<sup>2</sup>, J. Even<sup>1</sup>, and J.-M. Jancu<sup>1\*</sup>

<sup>1</sup>Université Européenne de Bretagne, INSA, FOTON, UMR 6082, 35708 Rennes, France

<sup>2</sup>Laboratoire de physico-chimie, des microstructures et des micro-systèmes, Institut Préparatoire aux Études Scientifiques et Techniques, Université de Carthage, BP51, 2070 La Marsa, Tunisie

## Abstract.

We report on semilocal and hybrid density functional theory (DFT) study of strained wurtzite crystals of InAs and InP. The crystal-field splitting has a large and non-linear dependence on strain for both crystals. Moreover, the study of the electronic deformation potentials reveals that the well-known quasi-cubic (QC) approximation fails to reproduce the non-ideal  $c/a$  ratio. This theoretical study is of crucial importance for the simulation of self-assembled InAs/InP nanowires.

\*Corresponding author: jean-marc.jancu@insa-rennes.fr

Semiconductor core/shell nanowires (NWs)<sup>1,2</sup> hold a lot of promises for applications in the field in electronics<sup>3,4</sup>, photonics<sup>5,6</sup>, and biochemical sensors.<sup>7</sup> These systems, compared to pure semiconductor wires, demonstrate a reduction of surface scattering and ionized impurity scattering<sup>8</sup> with improved electronic confinement properties. The synthesis process is mainly based on the gold-catalyzed vapor liquid-solid (VLS) growth mechanisms, which allows for a precise control of geometrical dimensions and strain accommodation.<sup>9</sup> The VLS method is particularly suited in interfacing highly strained III-V materials onto Si substrates.<sup>10</sup> Interestingly, it favors the hexagonal phase at the nucleation stage leading to a crystallization of III-V semiconductors in a hexagonal wurtzite (WZ) structure whereas the bulk counterpart for most of them is cubic zinc-blende (ZB).<sup>11</sup> Recently, much effort has been devoted to the growth and fabrication of strained InP/InAs/InPNW devices for the realization of high field-effect electron mobility transistors and circuits. Advantages of these systems include the high electron mobility ( $30\,000\text{ cm}^2/\text{V s}$  at 300 K) and velocity ( $43\,000\text{ cm/s}$ ) of InAs and a large conduction band offset between InAs and InP (0.5 eV).<sup>12</sup> Strain engineering is a well-established technique to tune the electronic band gap of nanostructures. For instance, the lattice mismatch of InAs on InP is about -3 % and it is expected to tailor the band offsets and carrier mobility by lifting the degeneracy in the electronic bands. In addition, strain effects can generate a piezoelectric polarization charge at interfaces leading to a band bending in the active region of the wire. Determining the materials properties of InAs/InP NWs is key to improving current generating efficiencies of underlying devices. The WZ and ZB band structures for bulk InAs and InP have been extensively studied both theoretically and experimentally.<sup>12-14</sup> Moreover, electronic deformation potentials (DPs) of cubic semiconductors are well documented in literature.<sup>12</sup> However, to the best of our knowledge, no work on DPs has dealt with WZ III-V materials so far. This first step is mandatory for realistic modeling of InAs/InP NWs in the WZ structure<sup>15</sup>, including the effects of linear and non-linear electro-elastic coupling.<sup>16</sup>

In this work, we perform *ab initio* calculations of deformation potentials in wurtzite InAs and InP. The structural relaxations with strain perturbations are performed using the plane-wave

projector augmented wave method (PAW) as implemented in the VASP code.<sup>17</sup> We used the Heyd-Scuseria-Ernzerhof (HSE06) DFT hybrid exchange correlation functional<sup>18,19</sup> with a screening parameter  $\mu=0.2$  and a mixing parameter of  $\alpha = 0.25$ . This approach has been found to give reliable results in group III-nitrides<sup>20</sup> and group II-oxides.<sup>21</sup> Generalized-Gradient Approximation (GGA) in the Perdew–Burke–Ernzerhof (PBE) parameterization<sup>22</sup> and single shot GW ( $G_0W_0$ ) calculations implemented in VASP are also performed for comparison. We used GGA eigenvalues as input to the single shot  $G_0W_0$  calculations leading to more reliable parameters such as band gap and deformation potentials. The semi-core  $d$ -electrons of In are treated as valence electrons. The procedure is carried out with a plane-wave cutoff of 600 eV and a 6x6x4 Monkhorst–Pack mesh for k-point sampling. This allows for a full relaxation of the structural parameters. The accuracy of the predicted equilibrium lattice constants for both InP and InAs correlates directly with the level of approximation in the functional as shown in Table I. HSE gives the most accurate results and the well-known overcorrection of GGA-PBE<sup>23</sup> becomes apparent. We also note in Tab. I that the WZ structure is not perfectly tetrahedral with non-ideal  $c/a$  and  $u$  (an ideal WZ lattice consists in a tetragonal ratio  $c/a=1.633$  of the lattice constants and an ideal internal cell parameter  $u=3/8$ ) as found for both simulations and experiment.

Fig. 1 shows the InAs and InP band structures at equilibrium near the  $\Gamma$ -point computed with HSE. Calculations are performed without spin-orbit coupling. The direct band gap is formed by an s-like  $\Gamma_{1c}(BC)$  conduction-band state and doubly degenerate p-like  $\Gamma_{6v}(HH, LH)$  and  $\Gamma_{1v}(CH)$  valence-band states. Two energy gaps can be defined according to the optical transitions:  $\Gamma_{6v} \rightarrow \Gamma_{1c}$  ( $A, B$ ) and  $\Gamma_{1v} \rightarrow \Gamma_{1c}$  ( $C$ ). In our simulations,  $E_{AB}$  is the fundamental transition energy for both InAs and InP. As evidenced in Fig. 1, away from the Brillouin zone-center, the valence bands are strongly admixed and their dispersion is non-parabolic. Therefore the valence-band effective masses cannot be easily derived for application in  $\mathbf{k}\cdot\mathbf{p}$  models. On the other hand, the conduction band energy dispersion is parabolic near the  $\Gamma$ -point and our HSE calculation of the electron masses perpendicular and parallel to the  $c$ -axis gives: 0.055 and 0.032 (in units of free

electron mass). These results are consistent with those of De and Prior obtained within an empirical pseudopotential approach.<sup>24</sup> As seen in Tab. I, the band-gap energy is sensitive to the details of the exchange and correlation functional and both the hybrid functional and single  $G_0W_0$  reproduce values close to the experimental data. Conversely, an equivalent crystal field splitting  $\Delta_{cr} = E_{HH} - E_{CH}$  is obtained for PBE and HSE and the value of InAs compares well with the self-consistent GW calculation of Zanoliet *al.*<sup>12,13</sup> A similar behavior between PBE and HSE for  $\Delta_{cr}$  under deformation is evidenced both for biaxial strain  $\varepsilon_{\perp}$  and for uniaxial strain  $\varepsilon_{zz}$  as shown in Fig. 2. As definition,  $\varepsilon_{\perp} = (\varepsilon_{xx} + \varepsilon_{yy})/2$  and  $\varepsilon_{zz}$  stand for the strain components in and perpendicular of the  $c$ -plane. In the calculations, the internal parameter  $u$  was fully relaxed for each strain. A nonlinear behavior is observed for the two semiconductors which can be interpolated with a polynomial regression. It should be noted that (Fig. 2b) HSE exhibits a strong nonlinearity for the crystal field splitting of InAs even for moderate biaxial strain.

The electronic deformation potentials are defined as the linear coefficients in the expansion of the  $\mathbf{k} \cdot \mathbf{p}$  band energies with respect to strain. We interpolated the present first-principle calculations for small deformations with a derivation of DPs from a 3x3 band  $\mathbf{k} \cdot \mathbf{p}$  model<sup>25</sup> which gives the linear dependence of  $E_{A/B}$  and  $E_C$  on strain as:

$$E_{A/B} = E_{A/B}(0) + (a_{cz} - D_1)\varepsilon_{zz} + (a_{ct} - D_2)\varepsilon_{\perp} - (D_3\varepsilon_{zz} + D_4\varepsilon_{\perp})$$

$$E_C = E_C(0) + (a_{cz} - D_1)\varepsilon_{zz} + (a_{ct} - D_2)\varepsilon_{\perp}$$

$(a_{cz}, a_{ct})$  and  $(D_1, D_2, D_3, D_4)$  characterize the deformation potentials of  $\Gamma_{1c}$  and  $\Gamma_{1v}$  and  $\Gamma_{6v}$  respectively. These relations are compatible with hexagonal symmetry  $C_{6v}$ . On the other hand, the breaking of symmetry  $C_{6v}$  to orthorhombic  $C_{2v}$  with in-plane anisotropic strain lifts the degeneracy of  $HH$  and  $LH$  levels as:

$$\Delta E = |E_{HH} - E_{CH}| = 2|D_5(\varepsilon_{xx} - \varepsilon_{yy})|$$

The electronic deformation potentials of WZ InAs and InP are listed in table II. Differences are

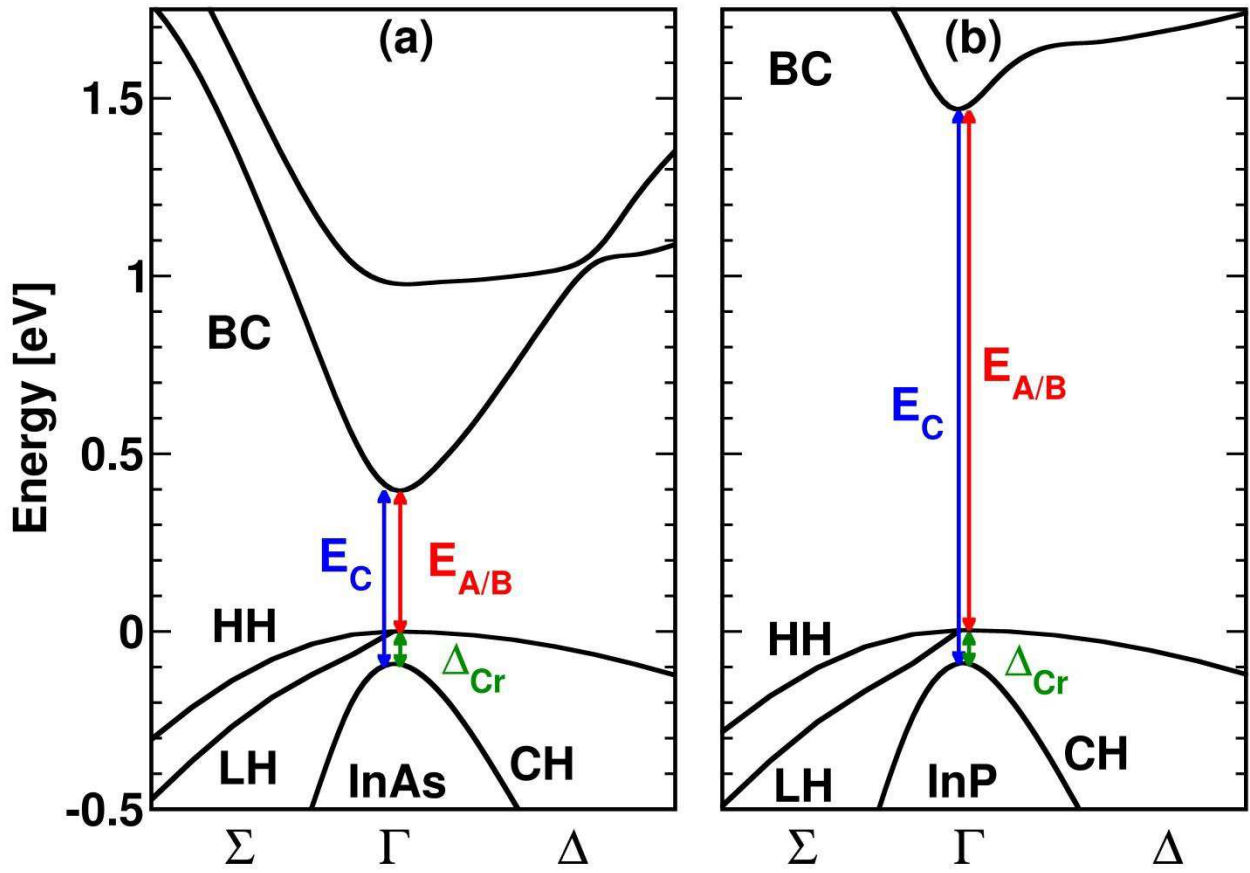
evidenced between PBE,  $G_0W_0$ , and HSE. However, the calculations ensure an overall uniform behavior for the DPs increasing distinctly from InAs to InP. This trend with the band-gap has been also observed in group III-nitrides<sup>20</sup> and group II-oxides.<sup>21</sup> Moreover, the band-gap-related deformation potentials of  $a_{cz}$ - $D_1$  and  $a_{cr}$ - $D_2$  are found more sensitive to exchange correlation functional than  $D_3$ ,  $D_4$  and  $D_5$ . Because there is currently no available experimental information and in order to gain insight into the quality of our simulations, we performed DP simulations in ZB InAs and InP as a test. By comparison to our previous DFT-LDA calculations<sup>26</sup>, HSE-based calculations lead to a better agreement with experiment. The same conclusion is drawn from our present GGA computation. This gives us confidence in the ability of the hybrid functional to model deformation potentials in wurtzite III-V semiconductors. Finally, the QC approximation was tested for InAs and InP from HSE results. The QC approximation is extensively used in  $\mathbf{k}\cdot\mathbf{p}$  Hamiltonians and based on a similar local atomic coordination between WZ and ZB crystals leading to a correlation of their physical properties along the [111] direction of the zinc-blende. Herein, we evaluated the deviation from the QC approximation of deformation potentials. Indeed, the same approximation in  $\mathbf{k}\cdot\mathbf{p}$  theory lead to:  $D_3 + 2D_4 = 0$  and  $D_1 + D_3 = D_2$ . Actually, neither for InAs nor InP satisfied these equations. For instance the first one yields -0.93 eV for InP and the failure must be related to the non-ideal  $c/a$  ratio.

As a conclusion, a systematic study of the electronic band structure in wurtzite InAs and InP is presented. Hybrid-functional calculations allow for a realistic description of the strained band energies. From accurate calculations of the electronic deformation potentials, we found the widely used QC approximation is not fulfilled for both InAs and InP. We demonstrated that the dependence of electronic bands on strain is strongly nonlinear and it should be taken into account for a proper modeling of InAs/InP nanowire-based devices.

This work was performed using HPC resources from GENCI CINES and IDRIS 2013-2013096724.

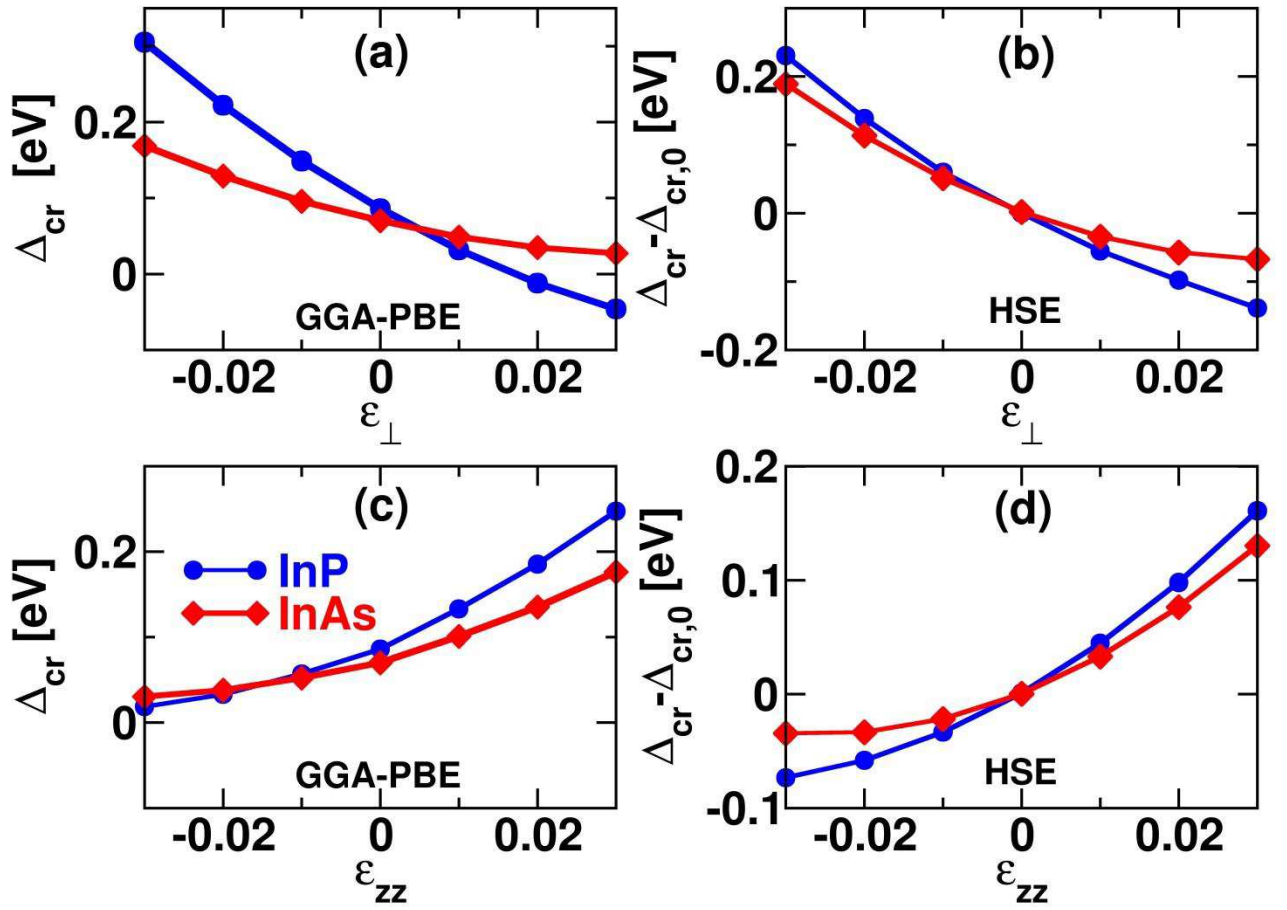
The work is supported through the participation of the INSCOOP ANR project

Figure captions.



**Figure 1:** Blow-up of the WZ-InAs (a) and WZ-InP (b) band structures calculated with HSE close to the  $\Gamma$  point.  $\Sigma$  and  $\Delta$  denote the in-plane and parallel directions with respect to  $c$ -axis. The origin of the energy scale is taken at the top of the valence band (VBM).





**Figure 2:** Left Panel:GGA-PBE dependence of the crystal-field splitting  $\Delta_{cr}(\epsilon)$  of InAs and InP on (a) in-plane and (c) perpendicular strain with respect to the c-plane. Right Panel: Dependence of  $\Delta_{cr}(\epsilon) - \Delta_{cr}(0)$  on (b) in-plane and (d) perpendicular strain calculated with HSE for InAs and InP. Quantization axis z is along the [0001] WZ direction.

## Tables.

**Table I:** Results of GGA-PBE, HSE, and  $G_0W_0$  calculations for wurtzite InAs and InP at equilibrium for the lattice constants ( $a$ ,  $c$ ), internal parameter  $u$ , direct band gap  $E_{A/B}$ , crystal-field splitting  $\Delta_{cr}$ , and compared with the experimental values<sup>2,14,27</sup> (Expt.). Single  $G_0W_0$  is performed on top of GGA calculations with identical structural parameters of GGA-PBE.

	Method	$a(\text{\AA})$	$c(\text{\AA})$	$u$	$E_{A/B}(\text{eV})$	$\Delta_{cr}(\text{eV})$
InP	PBE	4.229	6.881	0.3776	0.67	0.086
	$G_0W_0$				1.43	0.090
	HSE	4.174	6.824	0.3742	1.47	0.093
	Expt.	4.150 <sup>a</sup>	6.777 <sup>a</sup>	-	1.49 <sup>a</sup>	-
InAs	PBE	4.426	7.164	0.3817	-0.31	0.070
	$G_0W_0$				0.42	0.088
	HSE	4.330	7.066	0.3756	0.40	0.091
	Expt.	4.283 <sup>b</sup>	6.995 <sup>b</sup>	0.3750 <sup>b</sup>	0.52 <sup>c</sup>	-

<sup>a</sup> reference 27

<sup>b</sup>reference 14

<sup>c</sup> reference 2

**Table II:** Deformation potentials (eV) of wurtziteInAs and InP obtained with GGA-PBE,  $G_0W_0$ , and HSE.

	Method	$a_{cz} - D_1$	$a_{ct} - D_2$	$D_3$	$D_4$	$D_5$
InAs	PBE	-3.67	-5.31	4.70	-2.18	-2.21
	$G_0W_0$	-3.06	-6.12	5.62	-2.77	-2.63
	HSE	-2.69	-8.33	5.85	-3.17	-2.78
InP	PBE	-3.13	-7.20	5.55	-3.09	-2.84
	$G_0W_0$	-3.98	-7.43	5.67	-3.15	-2.88
	HSE	-4.05	-7.64	5.92	-3.28	-2.94

## References

- <sup>1</sup> F. Qian, Y. Li, S. Gradecak, H.G. Park, Y. Dong, Y. Ding, Z.L. Wang, and C.M. Lieber Nano Lett. **5**, 2287 (2005).
- <sup>2</sup> J. Bao, D. C. Bell, F. Capasso, N. Erdman, D. Wei, L. Froberg, T. Martensson, and L. Samuelson, Adv. Mater. **21**, 3654 (2009).
- <sup>3</sup> Y. Li, F. Qian, J. Xiang, and C. M. Lieber, Nature **441**, 489 (2006).
- <sup>4</sup> C. Thelander, P. Agarwal, S. Brongersma, J. Eymery, L. F. Feiner, A. Forchel, M. Scheffler, W. Riess, B. J. Ohlsson, U.Gösele, and L. Samuelson, Mater. Today **9**, 28 (2006).
- <sup>5</sup> X. Duan, Y. Huang, R. Agarwal, and C. M. Lieber, Nature **421**, 241 (2003).
- <sup>6</sup> M. H. Huang, S. Mao, H. Feick, H. Yan, Y. Wu, H. Kind, E. Weber, R. Russo, P. Yang, Science **292**, 1897 (2001).
- <sup>7</sup> Y. Cui, Q. Wei, H. Park, and C. M. Lieber, Science **293**, 1289 (2001).
- <sup>8</sup> J. W. W. van Tilburg, R. E. Algra, W. G. G. Immink, M. Verheijen, E. P. A. M. Bakkers, and L. P. Kouwenhoven, Semicond. Sci. Technol. **25**, 24011 (2010).
- <sup>9</sup> M. H. HadjAlouane, R. Anufriev, N. Chauvin, H. Khmissi, K. Naji, B. Ilahi, H. Maaref, G. Patriarche, M. Gendry, and C. Bru-Chevallier, Nanotechnology **22**, 405702 (2011).
- <sup>10</sup> M.H. HadjAlouane, N. Chauvin, H. Khmissi, K. Naji, B. Ilahi, H. Maaref, G. Patriarche, M. Gendry, and C. Bru-Chevallier, Nanotechnology **24**, 035704 (2013).
- <sup>11</sup> F. Glas, J-C. Harmand, and G. Patriarche, Phys. Rev. Lett. **99**, 146101 (2007).
- <sup>12</sup> I. Vurgaftman, J. R. Meyer, and L. R. Ram-Mohan, J. Appl. Phys. **89**, 5815 (2001).
- <sup>13</sup> Z. Zanolli, F. Fuchs, J. Furthmüller, U. von Barth, and F. Bechstedt, Phys. Rev. B **75**, 245121 (2007).
- <sup>14</sup> Z. Zanolli, M.-E. Pistol, L. E. Froberg, and L. Samuelson, J. Phys.: condens. Matter **19**, 295219 (2007).
- <sup>15</sup> J. Even, Appl. Phys. Lett. **94**, 102105 (2009).
- <sup>16</sup> L. Pedesseau, C. Katan, and J. Even, Appl. Phys. Lett. **100**, 031903 (2012).
- <sup>17</sup> G. Kresse and J. Furthmüller, Phys. Rev. B **54**, 11169 (1996).
- <sup>18</sup> J. Heyd, G. E. Scuseria, and M. Ernzerhof, J. Chem. Phys. **118**, 8207 (2003).
- <sup>19</sup> J. Heyd, G. E. Scuseria, and M. Ernzerhof, J. Chem. Phys. **124**, 219906 (2006).
- <sup>20</sup> Q. Yan, P. Rinke, M. Scheffler, and C. G. Van de Walle, Appl. Phys. Lett. **95**, 121111 (2009).
- <sup>21</sup> Q. Yan, P. Rinke, M. Winkelnkemper, A. Qteish, D. Bimberg, M. Scheffler, and C. G. Van de Walle, Appl. Phys. Lett. **101**, 152105 (2012).
- <sup>22</sup> J. P. Perdew, K. Burke, and M. Ernzerhof, Phys. Rev. Lett. **77**, 3865 (1996).
- <sup>23</sup> P. Haas, F. Tran, and P. Blaha, Phys. Rev. B **79**, 85104 (2009).
- <sup>24</sup> A. De and Craig E. Pryor, Phys. Rev. B **81**, 155210 (2010).
- <sup>25</sup> S. L. Chuang and C. S. Chang, Phys. Rev. B **54**, 2491 (1996).
- <sup>26</sup> L. Pedesseau, J. Even, A. Bondi, W. Guo, S. Richard, H. Folliot, C. Labbe, C. Cornet, O. Dehaese, A. Le Corre, O. Durand and S. Loualiche, J. Phys. D **41**, 165505 (2008).
- <sup>27</sup> J.-M. Jancu, K. Gauthron, L. Largeau, G. Patriarche, J.-C. Harmand, and P. Voisin, Appl. Phys. Lett. **97**, 41910 (2010).